The Ribosomal Operon Database (ROD): A full-length rDNA operon database derived from genome assemblies

Anders K. Krabberød*, Embla Stokke, Ella Thoen, Inger Skrede, Håvard Kauserud

Section for Genetics and Evolutionary Biology, Department of Biosciences, University of Oslo, Norway

*Corresponding author. Email: a.k.krabberod@ibv.uio.no

Abstract

Current rDNA reference sequence databases are tailored towards shorter DNA markers, such as parts of the 16/18S marker or the ITS region. However, due to advances in long-read DNA sequencing technologies, longer stretches of the rDNA operon are increasingly used in environmental sequencing studies to increase the phylogenetic resolution. There is, therefore, a growing need for longer rDNA reference sequences. Here, we present the Ribosomal Operon Database (ROD), which includes eukaryotic full-length rDNA operons fished from publicly available genome assemblies. Full-length operons were detected in 34.1% of the 34,701 examined eukaryotic genome assemblies from NCBI. In most cases (53.1%), more than one operon variant was detected, which can be due to intragenomic operon copy variability, allelic variation in non-haploid genomes, or technical errors from the sequencing and assembly process. The highest copy number found was 5,947 in *Zea mays*. In total, 453,697 unique operons were detected, with 69,480 operon variant clusters remaining after intragenomic clustering at 99% sequence identity. The operon length varied extensively across eukaryotes, ranging from 4,136 to 16,463 bp, which will lead to considerable PCR bias during amplification of the entire operon. Clustering the full-length operons revealed that the different parts (i.e., 18S, 28S, the hypervariable region V4 of 18S, and ITS) provide divergent taxonomic resolution, with 18S and the V4 region being the most conserved. The Ribosomal Operon Database (ROD) will be updated regularly to provide an increasing number of full-length rDNA operons to the scientific community.

Keywords: DNA metabarcoding; amplicon sequencing; environmental sequencing; reference sequences; ribosomal DNA

Introduction

DNA metabarcoding, high-throughput sequencing of short DNA regions amplified from environmental DNA followed by taxonomic annotation using known reference sequences, is a powerful approach to explore microbial communities (Taberlet et al., 2018). Different parts of the ribosomal rDNA operon are the predominant markers used in DNA metabarcoding studies, such as the V4 region commonly used for microeukaryotes (Hadziavdic et al., 2014; Krabberød et al., 2022; Logares et al., 2012) or the ITS regions commonly used for fungi (Schoch et al., 2012). In the last decade and a half, relatively short DNA markers within the 200-400 bp range have typically been used, mainly due to inherent length limitations of relevant sequencing technologies. For taxonomic annotation of these markers, designated sequence databases such as PR2 (Guillou et al., 2013), RDP (Maidak et al., 2001), SILVA (Quast et al., 2012), and UNITE (Nilsson et al., 2019) have been constructed, including millions of relatively short rDNA reference sequences.

In contrast to short-read DNA metabarcoding, long-read sequencing technologies make it possible to sequence longer stretches of the rDNA region (Jamy et al., 2020), even the entire rDNA operon (Wurzbacher et al., 2019), with high precision (Callahan et al., 2019). This calls for new reference sequences covering the whole rDNA operon. Comprehensive full-length operon databases have been developed for prokaryotes (Kerkhof et al., 2022; Seol et al., 2022) but not so far for eukaryotic organisms. One way to construct full-length operon reference sequences is to extract this information from genome assemblies; with increasing speed and precision, genome assemblies are becoming publicly available,

driven by large-scale initiatives such as the Earth Biogenome Project (Lewin et al., 2022), ERGA (Formenti et al., 2022) , Mycocosm (Grigoriev et al., 2014) and Darwin Tree of Life (Darwin Tree of Life Project Consortium, 2022). However, finding and extracting complete, full-length operons from genome assemblies can be difficult since technical errors may occur during sequencing and bioinformatics processing, rendering the ribosomal operon incomplete. Moreover, since the rDNA region is a multi-copy marker, intragenomic variants can exist (Lindner et al., 2013; Simon & Weiss, 2008) due to incomplete homogenization of the repeats (Elder & Turner, 1995; Ganley & Kobayashi, 2007).

Using longer stretches of the rDNA operon as a DNA metabarcoding marker can also pose extra challenges during PCR, partly due to its length, making it harder for the polymerase enzyme to read and copy the entire region. Moreover, various PCR biases, such as operon length differences among the target taxa, can skew the results. Although not thoroughly studied across the Eukaryotic Tree of Life, a considerable length variation occurs between lineages (Hall et al., 2022). One of the main reasons for this variation is introns, which have been shown to be prevalent in both 18S and 28S (Bhattacharya et al., 2000; Cannone et al., 2002; Hedberg & Johansen, 2013; Karpov et al., 2017).

Different parts of the rDNA operon mutate and evolve at different rates (Clark, 1987; Hall et al., 2022; Hillis & Dixon, 1991). Compared to the relatively conserved 18S and 28S regions, the ITS region evolves rapidly and can provide highly resolved taxonomic information down to the species level (Kauserud, 2023; Schoch et al., 2012). Different parts of the 18S and 28S genes also evolve at varying rates based on their position in the final rRNA molecule; in 18S, there are nine regions known to be hypervariable (named V1 to V9) (Hadziavdic et al., 2014; Nelles et al., 1984; Rajilić-Stojanović et al., 2009), while in 28S, there are twelve named D1-D12 (Chilton et al., 2003; Hassouna et al., 1984). These regions have different lengths and variability.

For instance, the V4 region in 18S shows significant sequence variability (Hadziavdic et al., 2014) and has been extensively used as a marker in DNA metabarcoding projects (Hadziavdic et al., 2014). D1, D2, and D3 of the 28S have similar properties and have been used to identify species where 18S has not provided the required taxonomic resolution (Douda et al., 2013; Qing et al., 2017; Rué et al., 2023; Sonnenberg et al., 2007). Knowing the level of variability and which taxonomic resolution the markers provide is crucial in DNA metabarcoding analyses. However, we have limited knowledge about the relative resolution of the different parts of the rDNA operon and how this may vary between taxonomic groups.

In this study, we introduce the full-length Ribosomal Operon Database (ROD) constructed from publicly available genome assemblies of eukaryotes. In addition to providing a high number of full-length operon reference sequences for the scientific community, we report on different features of the rDNA operons, including multiple operon variants in many genomes and length differences across eukaryotes. We also compare the level of molecular variation and how this affects the number of sequence clusters across different parts of the rDNA operon (18S, 28S, V4, ITS1, and ITS2), as well as the entire operon.

Materials and methods

Fishing reference operons

Initially, Barrnap (Seemann, n.d.) was used to identify the ribosomal RNA genes 18S, 5.8, and 28S from a selection of 947 genomes from Phycocosm (Grigoriev et al., 2021) and Mycocosm (Grigoriev et al., 2014). Following the initial identification, the output from Barrnap was analyzed to manually extract genomic regions where 18S, 5.8S, and 28S were arranged as a continuous operon on the same contig or scaffold, and a new Hidden Markov Model (HMM) was built to represent the complete operon. This model was constructed with hmmer3 (*HMMER 3.4 (Aug 2023)*, n.d.) from a MAFFT (Katoh & Standley, 2013)

alignment of 940 full-length ribosomal operons, representing a wide array of eukaryotic lineages and covering the major branches of the eukaryotic tree of life.

All eukaryotic genomes available in NCBI as of December 2023, in total 34,701, were downloaded and screened with the new full-length operon model using hmmscan. Regions matching the ribosomal operon were found in 17,107 of the genomes. To maintain the focus on complete, full-length operons, Barrnap (Seemann, n.d.) was used to search for operons with incomplete 18S or 28S; in the cases where either of these genes were marked as "partial," the operons were excluded from further analysis. After the filtration step, we were left with 453,697 operon sequences that we could say with reasonable confidence were full length.

Determining operon variants

We used VSEARCH (Rognes et al., 2016) to cluster full-length operons within each genome assembly at a 99% similarity threshold. This clustering aimed to eliminate potential technical errors from sequencing and assembly, and to identify operon variants that diverge by more than 1% in sequence identity. Operons that diverge by more than 1% in sequence identity are likely to represent biologically meaningful variants rather than just technical noise. Clustering at 99% allows these divergent operon variants to be distinguished and analyzed separately.

Eliminating contaminants

Several measures were taken to eliminate contaminants and incorrectly annotated genomes. This was done by comparing the centroid representatives from the clustered operons to the best hits in NCBI GenBank using blastn (Altschul et al., 1990). For each operon, 50 hits were retrieved from the NCBI nucleotide database and sorted by bitscore, e-value, and identity. The top hit for each query was then selected.

Taxonomic information was standardized using the R package *taxonomizr* (Sherrill-Mix, 2023) for both the retrieved genomes and the blast hit. The taxonomy identifier (TaxId) from the genomes in NCBI and the best hits for each centroid were used in the function *getTaxonomy(),* and the option for desired taxonomic levels was set to retrieve *superkingdom*, *kingdom*, *phylum*, *subphylum*, *class*, *order*, *family*, *genus*, and *species*. A comparative analysis of taxonomic assignments revealed possible discrepancies between the genome annotations and blast results, particularly in the higher taxonomic levels from *superkingdom* down to *order*. Operons with conflicting taxonomic assignments at these levels were excluded from the database to maintain its integrity. Additionally, operons with incomplete taxonomic information were quality-controlled by manually examining the top 50 blast hits, and a taxonomic assignment was selected to determine whether it was the majority among those matches. A total of 8614 centroids representing 34,015 ribosomal operons from 2,500 genomes were removed as contaminants. For 1,075 genomes, we uncovered one or more contaminant operons in addition to the operon corresponding to the expected taxonomy of the sequenced genome.

Streamlining taxonomy

Finally, the taxonomic assignments for the remaining operons were standardized to 9 different levels, following the setup in PR2 (Guillou et al., 2013). The levels used in ROD are *domain, supergroup division, subdivision, class, order, family, genus,* and *species*. The higher levels *domain*, *supergroup*, *division*, and *subdivision* correspond roughly to *superkingdom, kingdom, phylum,* and *subphylum* in NCBI but are adjusted to recent suggestions for the organization of the major branches of the Tree of Life (Adl et al., 2019; Burki et al., 2019). In addition to the taxonomic levels, ROD contains the GenBank *assembly_id* and the *taxid* from NCBI for each genome. After checking for length, clustering, and removing contaminants,

the database comprised 69,480 operon variants, representing 453,697 copies of the ribosomal operon from 11,935 genomes.

Genetic distance

The operon variants were aligned separately for each genome assembly with more than three variants using MAFFT (Katoh & Standley, 2013). After aligning, the genetic distance was calculated for each alignment using the *dist.dna()* function (Paradis & Schliep, 2019) with the TN93 model, which assumes distinct rates for both kinds of transition (A ↔ G versus C ↔ T) and transversions (Tamura & Nei, 1993), and the base rates were estimated from the data. The distance calculation was weighted by the geometric mean of the size of the variants, i.e.

$$D_{weigthed} = \frac{D_{original}}{\sqrt{size_A \times size_B}}$$

where $size_A$ and $size_B$ represent the copy number of two given operon variants and $D_{original}$ the unweighted genetic distance between the two. The average genetic distance was then calculated for each subdivision on the Tree of Life (Table 1).

Clustering analyses of sub-regions

To compare the level of molecular variation for the regions of the ribosomal operon often used in metabarcoding studies (Santoferrara, 2019), we extracted different parts (18S, 28S, V4, ITS1, and ITS2) from the entire operons and clustered these individually. To retrieve the regions, we first built an alignment of the operon variants using MAFFT. Next, we marked the boundaries of each region based on a set of primers and the identity score for the alignment. The primers used to identify the V4 region were 3NDf (Cavalier-Smith et al., 2009), and TAReukREV3 (Stoeck et al., 2010); the end of 18S (which is also the start of ITS1) was confirmed by EukB (Medlin et al., 1988), while the primer fITS7 was used to split ITS1 and ITS2 in 5.8S (Ihrmark et al., 2012). Finally, the beginning of 28S/end of ITS2 was confirmed with the primer ITS4 (White et al., 1990) (Fig. 1)

In addition to the 18S, 28S, ITS1, ITS2, and V4 subregion, a superregion encompassing ITS1-5.8S-ITS2 was also extracted and clustered. Full intragenomic operon centroids and subsectioned datasets were processed separately. Following an initial cleanup to remove sequences containing more than 20 consecutive N-bases in any subregion, the sequences were dereplicated and clustered using VSEARCH (Rognes et al. 2016). Clustering was performed from 95.0% to 100% with 0.5 increments to see the effect of different clustering levels for each subregion (Bonin et al., 2023).

Choosing a representative sequence

As a final resource, we chose one representative sequence from each genome assembly with the highest copy number of all the operon variants from a genome if more than one variant existed. In a few genome assemblies (68), two or more variants with the highest copy number were equally abundant, and they were not included in the reduced reference dataset in ROD.

Data visualization

Visualization of the number of genomes, operon variants, copy numbers, and genetic distance on the eukaryotic Tree of Life was done with the package *metacoder* (Foster et al., 2017) in R v4.3.3 (R Core Team, 2024). The ridgeplots were made in R with *ggplot2* (Wickham, 2016) and *ggridges* (Wilke, 2024), and the colors were based on the package *wesanderson* (Ram & Wickham, 2023).

Results

While a signal for the ribosomal operon was found in 17,107 out of the 34,701 genome assemblies, full-length rDNA operon(s) were detected in 11,935 genome assemblies (34.4%). The operons were clustered intragenomically at 99.0% sequence similarity to remove tentative technical errors from sequencing and assembly, as well as to record operon variants diverging by more than 1% in sequence identity. The number of clusters represents the number of operon variants per genome, and the size represents the number of copies found for a given variant. The set of operon variants (69,480), as well as a reference set including only the most abundant operon variant per genome (11,867), are available in the ROD database (https://github.com/krabberod/ROD). The release used in this study is ROD v1.0 (GoldenRod), which is also deposited on Zenodo (https://zenodo.org/records/10951604).

Figure 2 shows the distribution of the detected operons across major taxonomic groups. Fungi, which are intensively sequenced partly due to their small genomes, represent 55.5% of the genomes in ROD, followed by Metazoa (22.7%) and Viridiplantae (17.0%) (Fig. 2, Table 1). A single copy of the operon was found in 5,601 (46.9%) of the assemblies, while 53.1% had multiple copies. Among the genomes with multiple copies, most had between 2-10 copies (3,385), 2,241 had between 11 and 100 copies, 708 had more than 100 copies, and 92 genomes had more than 1,000 copies (Fig. 2). Most copies were observed in genome assemblies of Viridiplantae (Fig. 2, Table 1). The highest copy number, 5,947, was found in the genome of *Zea mays* (genome assembly id GCA_024505845 (Zhao et al., 2022)). Also, many Metazoa possessed several copies (Table 1), with the insect *Clusia tigrina* having the highest number with 4,691 copies (genome assembly id GCA_920105625 (Crowley et al., 2023)).

The number of operon variants per genome varied considerably between major taxonomic groups (Fig. 2). While 8,356 out of the 11,935 genome assemblies with a full-length operon had a single operon variant, 2,733 had between 2-10 variants, 730 between 11 and 100 variants, and 117 had more than 100 variants. As with the copy numbers, Viridiplantae included the most variant numbers (Fig. 2). Two plant species were the only genomes with more than 1000 operon variants: *Thlaspi arvense* with 1,017 variants (genome assembly id GCA_018983045 (Geng et al., 2021) and *Silybum marianum* with 2,097 variants (genome assembly id GCA_001541825.1 (Shim et al., 2023) (Table 1 and Supplementary table 1). In contrast, fungal genome assemblies generally had fewer variants; the highest number was 81, found in the ascomycete *Leptosphaeria maculans* (genome assembly id GCA_022343315 (Tian et al., 2024)).

To chart the amount of intragenomic variation, we calculated the genetic distance between all operon copies for each assembly separately (Fig. 2). Among the most abundant taxonomic groups sampled, Viridiplantae possessed the highest average genetic distance between copies (0.033). In comparison, the different sub-groups in Metazoa and Fungi had, on average, between 0.001-0.027 (Metazoa) and 0-0.12 (Fungi) sequence distance between copies (Table 1). The highest genetic divergence for a single assembly was observed in the assembly of the fungi *Neurospora* sp. CHS-2018c. Here, we found 30 operon variants, all single copies, with an average genetic distance of 0.215 (supplementary table 1).

The length of the operon varied extensively across the organismal groups (Fig. 3). The shortest operon found was 4,136 bp in the plant *Capsicum annuum* (assembly id GCA_030864225 (Estrada et al., 2024)), and the longest was 16,463 bp in the large bee-fly *Bombylius major* (assembly id GCA_932526495 (Lawniczak et al., 2023)). However, 86.0% of all operons had a length between 5,000 and 6,500 bp, and the median length was 5,779 bp (Fig. 3). Most of the operons in Fungi and Viridiplantae ranged between 5,500-6,100 bp in length (Fig. 3). The length variation was more extensive in Metazoa, where some groups, like Acanthocephala with an average operon length of 10,776 bp, possessed long operons.

To investigate the level of molecular variation across full-length operons compared to the 18S and 28S regions, as well as the shorter V4, ITS, ITS1, and ITS2 regions, and to understand how this variation influences cluster numbers, these regions were separately clustered across various sequence identity thresholds (Fig. 4a). Across all clustering thresholds, the 18S and V4 regions yielded the fewest clusters. In contrast, the more variable ITS region and the full-length operons produced the highest numbers (Fig. 4a).

Discussion

Recently, long-read sequencing approaches have been adopted in microbial ecology and DNA metabarcoding to obtain more detailed phylogenetic information about the microbial communities under investigation (Jamy et al., 2020, 2022; Tedersoo et al., 2020). More solid phylogenetic information is especially beneficial for poorly studied organisms that can be hard to place into a broader phylogenetic context (Krabberød et al., 2011). However, for long-read DNA metabarcoding analyses, we need reference sequences that cover longer stretches of the rDNA region, preferably the entire operon. Motivated by this, we provide full-length rDNA operon reference sequences assembled into the Ribosomal Operon Database (ROD). In addition to functioning as reference sequences for taxonomic annotation, the sequences in the ROD database may also fulfill other needs, such as reference sequences during chimera-checking, primer design, or phylogenetic binning. ROD currently includes 69,480 operon variants and their copy numbers extracted from 11,935 genomes. In addition, a reference set with only one operon (i.e., the most frequent) per genome is made available, which might be more useful in some investigations.

The reference sequence data have undergone multiple error correction steps, where contaminant and tentatively spurious sequences have been parsed out. Nevertheless, we cannot dismiss the possibility of spurious operons in the database. For example, we observed that many of the genome assemblies (29.3% of the full-length operons) were contaminated by other organisms. However, in this study, we only report on the observed operon variability in existing genome assemblies, and we do not aim to separate the different sources of variability.

We argue that full-length rDNA operon reference sequences should not be established based on concatenated sequences from different sub-parts, e.g., 18S and 28S, derived from multiple specimens, as this could lead to erroneous concatenation of different operon variants. Moreover, high-quality reference sequences should preferably be obtained from identified reference material, such as the sequencing of the full-length operon or genome from individuals in the case of multicellular organisms or axenic cultures in the case of single-celled organisms. Reference sequences obtained from environmental sequence data that have been assigned a taxonomy based on other reference sequences can also be useful but should be treated with caution since this represents indirect evidence. Moreover, a 'nearest neighbor' approach, in which the query sequence is assumed to have the same taxonomy as the closest match in a database, is highly dependent on the presence of a close match in the database or the training set (Murali et al., 2018). Adding to the dilemma, it is not always given how closely a sequence must match the reference in order to be correctly assigned to a given taxonomic rank, and the temptation to use the same naïve similarity cut-off for different groups of eukaryotes can easily lead to wrongful taxonomic annotations. In such cases, errors can quickly spread and multiply.

The copy number of the ribosomal operon can vary substantially between lineages of eukaryotes with as many as 19,300 reported in animals, more than 26,000 in plants (Prokopowich et al., 2003) and up to 1,442 in fungi (Lofgren et al., 2019). There are much fewer genomes available from microbial eukaryotes (protists). It has been shown, however, that many protist groups have a huge number of copies. In Foraminfera, the average number varies between 4,000 and 50,000 in different species (Milivojević et al.,

255 2021), while the ciliate *Halteria grandinella* has as many as 567,893 copies (Wang et al., 2017). The
256 number of copies can even vary between individuals of the same species, and this variation in copy number
257 has been reported to result from both genetic and environmental factors (Lavrinienko et al., 2021;
258 Milivojević et al., 2021; Symonová, 2019). Reports on copy number variation are mostly done with qPCR
259 or other cytological measurements, and such high numbers seldom occur in genome assembly projects. The
260 reason is that until recently, repeated elements were very hard to resolve accurately due to the short read
261 length of the sequencing platforms (Tørresen et al., 2019). In genome assemblies based on short reads,
262 repeated elements tend to collapse into one representative sequence, and the number of actual copies per
263 genome reported in the current version of ROD is, therefore, likely an underestimate. With the advent of
264 highly accurate long-read sequencing technologies, the possibility of resolving long repeats is increasing
265 and will most likely improve in the future.

266 It is commonly known that copies are usually found in tandem repeats, and concerted evolution mechanisms
267 keep the copies highly uniform (Eickbush & Eickbush, 2007). However, multiple operon variants, here
268 defined as operons diverging by more than 1% in sequence identity, were discovered in approximately 30%
269 of the genomes analyzed. Especially in the analyzed plant genomes, we observed a high number of operon
270 variants per genome, which could be due to their often polyploid nature. But even in haploid genomes,
271 multiple variants can be expected if the multiple operon copies are not homogenized by concerted evolution
272 (Bradshaw et al., 2023). The occurrence of multiple, divergent operon variants per genome (or individuals)
273 can lead to inflation of the diversity (Lavrinienko et al., 2021; Thornhill et al., 2007). Operons can
274 occasionally appear in genome assemblies as multiple variants for technical reasons. Our analysis showed
275 that more than 50% of the genomes from NCBI had ribosomal operons from contaminating species. These
276 can readily be removed by blasting and comparing the taxonomic affiliation of the sequence to the expected
277 taxonomy of the genome being assembled. These issues can be difficult to resolve, but as sequencing
278 platforms improve and sequences become longer and more accurate, these problems are expected to be
279 improved. Thanks to advancements in sequencing and bioinformatics methods, we envision that future
280 genome assemblies will be of even higher quality.

281 Using the full ROD dataset as reference sequences for environmental sequencing studies can help address
282 the issue of multiple operon variants during the taxonomic annotation process. This might be especially
283 important for organismal groups with divergent operons, such as Viridiplantae. Due to the initial 99%
284 clustering of operons within each genome, we may underestimate the true variant numbers.

285 High variation in the operon copy number was observed across the eukaryotic tree of life, with an average
286 high copy number present in Viridiplantae. The copy number variability will introduce PCR bias in DNA
287 metabarcoding projects with environmental samples, where genomes and taxa with high copy number will
288 be preferentially amplified (Lavrinienko et al., 2021). If the copy number variability becomes better known,
289 measures may be taken to account for this bias in the final data (Stoddard et al., 2015)

290 Significant operon length differences are present between and within various taxonomic groups. Based on
291 our data, the length variability seems especially prominent in Metazoa. One major cause for the extremely
292 long variants is the presence of introns in several lineages (Bhattacharya et al., 2000; Chang et al., 2017;
293 Hedberg & Johansen, 2013; Karpov et al., 2017). During the amplification of longer stretches or the entirety
294 of the rDNA operon, the length differences will introduce PCR bias, where taxa with shorter variants will
295 be preferentially amplified. In theory, if the length variation is known across organismal groups, the bias
296 could be modeled and taken into account.

297 Due to the varying rates of molecular evolution across the rDNA operon, different regions provide different
298 phylogenetic and taxonomic resolutions. This variation is further complicated by differing evolutionary

rates in rDNA operons across the Tree of Life, making the selection of optimal barcoding regions and clustering settings for operational taxonomic units (OTUs) a significant challenge (Phillips et al., 2022). For example, while the ITS region frequently offers species-level resolution for fungi (Schoch et al., 2012), using more conserved markers such as V4 often groups related species into the same OTUs at the same clustering level. Our clustering analyses show that both the ITS regions and the entire operon provide more fine-grained taxonomic resolution than 18S and the hypervariable region V4. These findings indicate the necessity for marker-specific bioinformatic processing strategies, including adjusting clustering levels to avoid potential over-splitting or merging sequences during OTU construction (Bonin et al., 2023; He et al., 2015).

The ROD database currently possesses a taxonomically highly skewed collection of reference sequences that reflect the distribution of available genomes in NCBI. Fungi are the dominating group, followed by Metazoa and Viridiplantae. Due to their small genome size and biotechnological importance, many fungal genomes have been sequenced and are available in public databases (de Vries et al., 2018; Xu, 2023). In the future, we expect more genomes from neglected branches on the Tree of Life distribution, including more protist genomes. Due to advances in single-cell genomics, genomes from single-celled protists will expectedly become more available as references (Sieracki et al., 2019). Because of the steadily increasing pace of genome sequencing, we expect a strong increase in the number of operons that will become available for inclusion in ROD in the near future. We intend to provide regularly updated versions of ROD.

Acknowledgments

We would like to thank Ane-Rikke N. Oenting for invaluable feedback, the University of Oslo for financial support, and the National Infrastructure for High-Performance Computing in Norway (Sigma2) for access to computational resources on projects NN9338K, NN9725K, and NN9699K.

References

Adl, S. M., Bass, D., Lane, C. E., Lukeš, J., Schoch, C. L., Smirnov, A., Agatha, S., Berney, C., Brown, M. W., Burki, F., Cárdenas, P., Čepička, I., Chistyakova, L., Del Campo, J., Dunthorn, M., Edvardsen, B., Eglit, Y., Guillou, L., Hampl, V., … Zhang, Q. (2019). Revisions to the classification, nomenclature, and diversity of eukaryotes. *The Journal of Eukaryotic Microbiology*, *66*(1), 4–119. https://doi.org/10.1111/jeu.12691

Altschul, S. F., Gish, W., Miller, W., Myers, E. W., & Lipman, D. J. (1990). Basic local alignment search tool. *Journal of Molecular Biology*, *215*(3), 403–410. https://doi.org/10.1016/S0022-2836(05)80360-2

Bhattacharya, D., Lutzoni, F., Reeb, V., Simon, D., Nason, J., & Fernandez, F. (2000). Widespread occurrence of spliceosomal introns in the rDNA genes of Ascomycetes. *Molecular Biology and Evolution*, *17*(12), 1971–1984. https://doi.org/10.1093/oxfordjournals.molbev.a026298

Bonin, A., Guerrieri, A., & Ficetola, G. F. (2023). Optimal sequence similarity thresholds for clustering of molecular operational taxonomic units in DNA metabarcoding studies. *Molecular Ecology Resources*, *23*(2), 368–381. https://doi.org/10.1111/1755-0998.13709

Bradshaw, M. J., Aime, M. C., Rokas, A., Maust, A., Moparthi, S., Jellings, K., Pane, A. M., Hendricks, D., Pandey, B., Li, Y., & Pfister, D. H. (2023). Extensive intragenomic variation in the internal transcribed spacer region of fungi. *IScience*, *26*(8), 107317. https://doi.org/10.1016/j.isci.2023.107317

Burki, F., Roger, A. J., Brown, M. W., & Simpson, A. G. B. (2019). The new tree of eukaryotes. *Trends in Ecology & Evolution*, *35*(1), 43–55. https://doi.org/10.1016/j.tree.2019.08.008

Callahan, B. J., Wong, J., Heiner, C., Oh, S., Theriot, C. M., Gulati, A. S., McGill, S. K., & Dougherty, M. K. (2019). High-throughput amplicon sequencing of the full-length 16S rRNA gene with single-nucleotide resolution. *Nucleic Acids Research*, *47*(18), e103–e103. https://doi.org/10.1093/nar/gkz569

Cannone, J. J., Subramanian, S., Schnare, M. N., Collett, J. R., D'Souza, L. M., Du, Y., Feng, B., Lin, N., Madabusi, L. V., Müller, K. M., Pande, N., Shang, Z., Yu, N., & Gutell, R. R. (2002). The comparative RNA web (CRW) site: an online database of comparative sequence and structure information for ribosomal, intron, and other RNAs. *BMC Bioinformatics*, *3*, 2. https://doi.org/10.1186/1471-2105-3-2

Cavalier-Smith, T., Lewis, R., Chao, E. E., Oates, B., & Bass, D. (2009). *Helkesimastix marina* n. sp. (Cercozoa: Sainouroidea superfam. n.) a gliding zooflagellate of novel ultrastructure and unusual ciliary behaviour. *Protist*, *160*(3), 452–479. https://doi.org/10.1016/j.protis.2009.03.003

Chang, N., Sun, Q., Hu, J., An, C., & Gao, H. (2017). Large introns of 5 to 10 kilo base pairs can be spliced out in Arabidopsis. *Genes*, *8*(8). https://doi.org/10.3390/genes8080200

Chilton, N. B., Huby-Chilton, F., & Gasser, R. B. (2003). First complete large subunit ribosomal RNA sequence and secondary structure for a parasitic nematode: phylogenetic and diagnostic implications. *Molecular and Cellular Probes*, *17*(1), 33–39. https://doi.org/10.1016/s0890-8508(02)00107-x

Clark, C. G. (1987). On the evolution of ribosomal RNA. *Journal of Molecular Evolution*, *25*(4), 343–350. https://doi.org/10.1007/bf02603119

Crowley, L. M., Akinmusola, R. Y., University of Oxford and Wytham Woods Genome Acquisition Lab, Darwin Tree of Life Barcoding collective, Wellcome Sanger Institute Tree of Life programme, Wellcome Sanger Institute Scientific Operations: DNA Pipelines collective, Tree of Life Core Informatics collective, & Darwin Tree of Life Consortium. (2023). The genome sequence of a druid fly, *Clusia tigrina* (Fallén, 1820). *Wellcome Open Research*, *8*, 430. https://doi.org/10.12688/wellcomeopenres.20109.1

Darwin Tree of Life Project Consortium. (2022). Sequence locally, think globally: The Darwin Tree of Life Project. *Proceedings of the National Academy of Sciences of the United States of America*, *119*(4), e2115642118. https://doi.org/10.1073/pnas.2115642118

de Vries, R. P., Grigoriev, I. V., & Tsang, A. (2018). Introduction: Overview of fungal genomics. In *Methods in Molecular Biology* (Vol. 1775, pp. 1–7). Springer New York. https://doi.org/10.1007/978-1-4939-7804-5_1

Douda, O., Marek, M., Zouhar, M., & Ryšánek, P. (2013). Insights into the structure and phylogeny of the 28S rRNA expansion segments D2 and D3 of the plant-infecting nematodes from the genus Ditylenchus (Nematoda: Anguinidae). *Phytopathol. Mediterr.*, *52*, 84–97. https://doi.org/10.14601/PHYTOPATHOL_MEDITERR-11334

Eickbush, T. H., & Eickbush, D. G. (2007). Finely orchestrated movements: evolution of the ribosomal RNA genes. *Genetics*, *175*(2), 477–485. https://doi.org/10.1534/genetics.107.071399

Elder, J. F., Jr, & Turner, B. J. (1995). Concerted evolution of repetitive DNA sequences in eukaryotes. *The Quarterly Review of Biology*, *70*(3), 297–320. https://doi.org/10.1086/419073

Estrada, R., Tantalean, J. F. C., Saldaña, C. L., Romero, Y., Vilcara, E., & Arbizu, C. I. (2024). Draft genome and SSR data mining of a Peruvian landrace of *Capsicum chinense*, the arnaucho chili pepper. *Genet. Resour. Crop Evol.* https://doi.org/10.1007/s10722-024-01941-4

Formenti, G., Theissinger, K., Fernandes, C., Bista, I., Bombarely, A., Bleidorn, C., Ciofi, C., Crottini, A., Godoy, J. A., Höglund, J., Malukiewicz, J., Mouton, A., Oomen, R. A., Paez, S., Palsbøll, P. J., Pampoulie, C., Ruiz-López, M. J., Svardal, H., Theofanopoulou, C., … European Reference Genome Atlas (ERGA) Consortium. (2022). The era of reference genomes in conservation genomics. *Trends in Ecology & Evolution*, *37*(3), 197–202. https://doi.org/10.1016/j.tree.2021.11.008

Foster, Z. S. L., Sharpton, T. J., & Grünwald, N. J. (2017). Metacoder: An R package for visualization and manipulation of community taxonomic diversity data. *PLoS Computational Biology*, *13*(2), e1005404. https://doi.org/10.1371/journal.pcbi.1005404

Ganley, A. R. D., & Kobayashi, T. (2007). Highly efficient concerted evolution in the ribosomal DNA repeats: total rDNA repeat variation revealed by whole-genome shotgun sequence data. *Genome Research*, *17*(2), 184–191. https://doi.org/10.1101/gr.5457707

Geng, Y., Guan, Y., Qiong, L., Lu, S., An, M., Crabbe, M. J. C., Qi, J., Zhao, F., Qiao, Q., & Zhang, T. (2021). Genomic analysis of field pennycress (*Thlaspi arvense*) provides insights into mechanisms of adaptation to high elevation. *BMC Biology*, *19*(1), 143. https://doi.org/10.1186/s12915-021-01079-0

Grigoriev, I. V., Hayes, R. D., Calhoun, S., Kamel, B., Wang, A., Ahrendt, S., Dusheyko, S., Nikitin, R., Mondo, S. J., Salamov, A., Shabalov, I., & Kuo, A. (2021). PhycoCosm, a comparative algal genomics resource. *Nucleic Acids Research*, *49*(D1), D1004–D1011. https://doi.org/10.1093/nar/gkaa898

Grigoriev, I. V., Nikitin, R., Haridas, S., Kuo, A., Ohm, R., Otillar, R., Riley, R., Salamov, A., Zhao, X., Korzeniewski, F., Smirnova, T., Nordberg, H., Dubchak, I., & Shabalov, I. (2014). MycoCosm portal: gearing up for 1000 fungal genomes. *Nucleic Acids Research*, *42*(Database issue), D699-704. https://doi.org/10.1093/nar/gkt1183

Guillou, L., Bachar, D., Audic, S., Bass, D., Berney, C., Bittner, L., Boutte, C., Burgaud, G., Vargas, C. de, Decelle, J., Campo, J. D., Dolan, J. R., Dunthorn, M., Edvardsen, B., Holzmann, M., Kooistra, W. H., Lara, E., Bescot, N. L., Logares, R., … Christen, R. (2013). The Protist Ribosomal Reference database (PR2): a catalog of unicellular eukaryote small sub-unit rRNA sequences with curated taxonomy. *Nucleic Acids Research*, *41*(Database issue), D597-604. https://doi.org/10.1093/nar/gks1160

Hadziavdic, K., Lekang, K., Lanzen, A., Jonassen, I., Thompson, E. M., & Troedsson, C. (2014). Characterization of the 18S rRNA gene for designing universal eukaryote specific primers. *PloS One*, *9*(2), e87624. https://doi.org/10.1371/journal.pone.0087624

Hall, A. N., Morton, E., & Queitsch, C. (2022). First discovered, long out of sight, finally visible: ribosomal DNA. *Trends in Genetics: TIG*, *38*(6), 587–597. https://doi.org/10.1016/j.tig.2022.02.005

Hassouna, N., Michot, B., & Bachellerie, J. P. (1984). The complete nucleotide sequence of mouse 28S rRNA gene. Implications for the process of size increase of the large subunit rRNA in higher eukaryotes. *Nucleic Acids Research*, *12*(8), 3563–3583. https://doi.org/10.1093/nar/12.8.3563

He, Y., Caporaso, J. G., Jiang, X.-T., Sheng, H.-F., Huse, S. M., Rideout, J. R., Edgar, R. C., Kopylova, E., Walters, W. A., Knight, R., & Zhou, H.-W. (2015). Stability of operational taxonomic units: an important but neglected property for analyzing microbial diversity. *Microbiome*, *3*(1), 20. https://doi.org/10.1186/s40168-015-0081-x

Hedberg, A., & Johansen, S. D. (2013). Nuclear group I introns in self-splicing and beyond. *Mobile DNA*, *4*(1), 17. https://doi.org/10.1186/1759-8753-4-17

419 Hillis, D. M., & Dixon, M. T. (1991). Ribosomal DNA: molecular evolution and phylogenetic inference.
420 *The Quarterly Review of Biology*, *66*(4), 411–453. https://doi.org/10.1086/417338

421 *HMMER 3.4 (Aug 2023)*. (n.d.). HMMER. http://hmmer.org/

422 Ihrmark, K., Bödeker, I. T. M., Cruz-Martinez, K., Friberg, H., Kubartova, A., Schenck, J., Strid, Y.,
423 Stenlid, J., Brandström-Durling, M., Clemmensen, K. E., & Lindahl, B. D. (2012). New primers to amplify
424 the fungal ITS2 region - evaluation by 454-sequencing of artificial and natural communities. *FEMS*
425 *Microbiology Ecology*, *82*(3), 666–677. https://doi.org/10.1111/j.1574-6941.2012.01437.x

426 Jamy, M., Biwer, C., Vaulot, D., Obiol, A., Jing, H., Peura, S., Massana, R., & Burki, F. (2022). Global
427 patterns and rates of habitat transitions across the eukaryotic tree of life. *Nature Ecology & Evolution*, 1–
428 13. https://doi.org/10.1038/s41559-022-01838-4

429 Jamy, M., Foster, R., Barbera, P., Czech, L., Kozlov, A., Stamatakis, A., Bending, G., Hilton, S., Bass, D.,
430 & Burki, F. (2020). Long-read metabarcoding of the eukaryotic rDNA operon to phylogenetically and
431 taxonomically resolve environmental diversity. *Molecular Ecology Resources*, *20*(2), 429–443.
432 https://doi.org/10.1111/1755-0998.13117

433 Karpov, S. A., Mamanazarova, K. S., Popova, O. V., Aleoshin, V. V., James, T. Y., Mamkaeva, M. A.,
434 Tcvetkova, V. S., Vishnyakov, A. E., & Longcore, J. E. (2017). *Monoblepharidomycetes* diversity includes
435 new parasitic and saprotrophic species with highly intronized rDNA. *Fungal Biology*, *121*(8), 729–741.
436 https://doi.org/10.1016/j.funbio.2017.05.002

437 Katoh, K., & Standley, D. M. (2013). MAFFT multiple sequence alignment software version 7:
438 improvements in performance and usability. *Molecular Biology and Evolution*, *30*(4), 772–780.
439 https://doi.org/10.1093/molbev/mst010

440 Kauserud, H. (2023). ITS alchemy: On the use of ITS as a DNA marker in fungal ecology. *Fungal Ecology*,
441 *65*(101274), 101274. https://doi.org/10.1016/j.funeco.2023.101274

442 Kerkhof, L. J., Roth, P. A., Deshpande, S. V., Bernhards, R. C., Liem, A. T., Hill, J. M., Häggblom, M. M.,
443 Webster, N. S., Ibironke, O., Mirzoyan, S., Polashock, J. J., & Sullivan, R. F. (2022). A ribosomal operon
444 database and MegaBLAST settings for strain-level resolution of microbiomes. *FEMS Microbes*, *3*, xtac002.
445 https://doi.org/10.1093/femsmc/xtac002

446 Krabberød, A. K., Bråte, J., Dolven, J. K., Ose, R. F., Klaveness, D., Kristensen, T., Bjørklund, K. R., &
447 Shalchian-Tabrizi, K. (2011). Radiolaria divided into Polycystina and Spasmaria in combined 18S and 28S
448 rDNA phylogeny. *PloS One*, *6*(8), e23526–e23526. https://doi.org/10.1371/journal.pone.0023526

449 Krabberød, A. K., Deutschmann, I. M., Bjorbækmo, M. F. M., Balagué, V., Giner, C. R., Ferrera, I., Garcés,
450 E., Massana, R., Gasol, J. M., & Logares, R. (2022). Long-term patterns of an interconnected core marine
451 microbiota. *Environmental Microbiome*, *17*(1), 2021.03.18.435965. https://doi.org/10.1186/s40793-022-
452 00417-1

453 Lavrinienko, A., Jernfors, T., Koskimäki, J. J., Pirttilä, A. M., & Watts, P. C. (2021). Does intraspecific
454 variation in rDNA copy number affect analysis of microbial communities? *Trends in Microbiology*, *29*(1),
455 19–27. https://doi.org/10.1016/j.tim.2020.05.019

456 Lawniczak, M. K. N., Crowley, L. M., McAlister, E., University of Oxford and Wytham Woods Genome
457 Acquisition Lab, Darwin Tree of Life Barcoding collective, Wellcome Sanger Institute Tree of Life
458 programme, Wellcome Sanger Institute Scientific Operations: DNA Pipelines collective, Tree of Life Core

Informatics collective, & Darwin Tree of Life Consortium. (2023). The genome sequence of the dark-edged bee fly, *Bombylius major* (Linnaeus, 1758). *Wellcome Open Research*, *8*, 379. https://doi.org/10.12688/wellcomeopenres.19804.1

Lewin, H. A., Richards, S., Aiden, E. L., Allende, M. L., Archibald, J. M., Bálint, M., Barker, K. B., Baumgartner, B., Belov, K., Bertorelle, G., Blaxter, M. L., Cai, J., Caperello, N. D., Carlson, K., Castilla-Rubio, J. C., Chaw, S.-M., Chen, L., Childers, A. K., Coddington, J. A., … Zhang, G. (2022). The Earth BioGenome Project 2020: Starting the clock. *Proceedings of the National Academy of Sciences*, *119*(4), e2115635118. https://doi.org/10.1073/pnas.2115635118

Lindner, D. L., Carlsen, T., Henrik Nilsson, R., Davey, M., Schumacher, T., & Kauserud, H. (2013). Employing 454 amplicon pyrosequencing to reveal intragenomic divergence in the internal transcribed spacer rDNA region in fungi. *Ecology and Evolution*, *3*(6), 1751–1764. https://doi.org/10.1002/ece3.586

Lofgren, L. A., Uehling, J. K., Branco, S., Bruns, T. D., Martin, F., & Kennedy, P. G. (2019). Genome-based estimates of fungal rDNA copy number variation across phylogenetic scales and ecological lifestyles. *Molecular Ecology*, *28*(4), 721–730. https://doi.org/10.1111/mec.14995

Logares, R., Haverkamp, T. H. A., Kumar, S., Lanzén, A., Nederbragt, A. J., Quince, C., & Kauserud, H. (2012). Environmental microbiology through the lens of high-throughput DNA sequencing: synopsis of current platforms and bioinformatics approaches. *Journal of Microbiological Methods*, *91*(1), 106–113. https://doi.org/10.1016/j.mimet.2012.07.017

Maidak, B. L., Cole, J. R., Lilburn, T. G., Parker, C. T., Jr, Saxman, P. R., Farris, R. J., Garrity, G. M., Olsen, G. J., Schmidt, T. M., & Tiedje, J. M. (2001). The RDP-II (Ribosomal Database Project). *Nucleic Acids Research*, *29*(1), 173–174. https://doi.org/10.1093/nar/29.1.173

Medlin, L., Elwood, H. J., Stickel, S., & Sogin, M. L. (1988). The characterization of enzymatically amplified eukaryotic 16S-like rRNA-coding regions. *Gene*, *71*(2), 491–499. https://doi.org/10.1016/0378-1119(88)90066-2

Milivojević, T., Rahman, S. N., Raposo, D., Siccha, M., Kucera, M., & Morard, R. (2021). High variability in SSU rDNA gene copy number among planktonic foraminifera revealed by single-cell qPCR. *ISME Communications*, *1*(1), 63. https://doi.org/10.1038/s43705-021-00067-3

Murali, A., Bhargava, A., & Wright, E. S. (2018). IDTAXA: a novel approach for accurate taxonomic classification of microbiome sequences. *Microbiome*, *6*(1), 140. https://doi.org/10.1186/s40168-018-0521-5

Nelles, L., Fang, B.-L., Volckaert, G., Vandenberghe, A., & Wachter, R. D. (1984). Nucleotide sequence of a crustacean 18S ribosomal RNA gene and secondary structure of eukaryotic small subunit ribosoraal RNAs. *Nucleic Acids Research*, *12*(23), 8749–8768. https://doi.org/10.1093/nar/12.23.8749

Nilsson, R. H., Larsson, K.-H., Taylor, A. F. S., Bengtsson-Palme, J., Jeppesen, T. S., Schigel, D., Kennedy, P., Picard, K., Glöckner, F. O., Tedersoo, L., Saar, I., Kõljalg, U., & Abarenkov, K. (2019). The UNITE database for molecular identification of fungi: handling dark taxa and parallel taxonomic classifications. *Nucleic Acids Research*, *47*(D1), D259–D264. https://doi.org/10.1093/nar/gky1022

Paradis, E., & Schliep, K. (2019). ape 5.0: an environment for modern phylogenetics and evolutionary analyses in R. *Bioinformatics (Oxford, England)*, *35*(3), 526–528. https://doi.org/10.1093/bioinformatics/bty633

Phillips, J. D., Gillis, D. J., & Hanner, R. H. (2022). Lack of statistical rigor in DNA barcoding likely invalidates the presence of a true species' barcode gap. *Frontiers in Ecology and Evolution*, *10*. https://doi.org/10.3389/fevo.2022.859099

Prokopowich, C. D., Gregory, T. R., & Crease, T. J. (2003). The correlation between rDNA copy number and genome size in eukaryotes. *Genome*, *46*(1), 48–50. https://doi.org/10.1139/g02-103

Qing, X., Slos, D., Claeys, M., & Bert, W. (2017). Ultrastructural, phylogenetic and rRNA secondary structural analysis of a new nematode (Nematoda: Tylenchomorpha) from mushroom with recovery of intestinal crystals. *Zoologischer Anzeiger*, *269*, 13–25. https://doi.org/10.1016/j.jcz.2017.06.002

Quast, C., Pruesse, E., Yilmaz, P., Gerken, J., Schweer, T., Yarza, P., Peplies, J., & Glöckner, F. O. (2012). The SILVA ribosomal RNA gene database project: improved data processing and web-based tools. *Nucleic Acids Research*, *41*(D1), D590–D596. https://doi.org/10.1093/nar/gks1219

R Core Team. (2024). *R: A Language and Environment for Statistical Computing*. R Foundation for Statistical Computing. https://www.R-project.org/

Rajilić-Stojanović, M., Heilig, H. G. H. J., Molenaar, D., Kajander, K., Surakka, A., Smidt, H., & De Vos, W. M. (2009). Development and application of the human intestinal tract chip, a phylogenetic microarray: analysis of universally conserved phylotypes in the abundant microbiota of young and elderly adults. *Environmental Microbiology*, *11*(7), 1736–1751. https://doi.org/10.1111/j.1462-2920.2009.01900.x

Ram, K., & Wickham, H. (2023). *wesanderson: A Wes Anderson Palette Generator*. https://CRAN.R-project.org/package=wesanderson

Rognes, T., Flouri, T., Nichols, B., Quince, C., & Mahé, F. (2016). VSEARCH: a versatile open source tool for metagenomics. *PeerJ*, *4*, e2584. https://doi.org/10.7717/peerj.2584

Rué, O., Coton, M., Dugat-Bony, E., Howell, K., Irlinger, F., Legras, J.-L., Loux, V., Michel, E., Mounier, J., Neuvéglise, C., & Sicard, D. (2023). Comparison of metabarcoding taxonomic markers to describe fungal communities in fermented foods. In *bioRxiv*. https://doi.org/10.1101/2023.01.13.523754

Santoferrara, L. F. (2019). Current practice in plankton metabarcoding: optimization and error management. *Journal of Plankton Research*, *41*(5), 571–582. https://doi.org/10.1093/plankt/fbz041

Schoch, C. L., Seifert, K. A., Huhndorf, S., Robert, V., Spouge, J. L., Levesque, C. A., Chen, W., Fungal Barcoding Consortium, & Fungal Barcoding Consortium Author List. (2012). Nuclear ribosomal internal transcribed spacer (ITS) region as a universal DNA barcode marker for Fungi. *Proceedings of the National Academy of Sciences of the United States of America*, *109*(16), 6241–6246. https://doi.org/10.1073/pnas.1117018109

Seemann, T. (n.d.). *barrnap: Bacterial ribosomal RNA predictor*. Retrieved February 23, 2024, from https://github.com/tseemann/barrnap

Seol, D., Lim, J. S., Sung, S., Lee, Y. H., Jeong, M., Cho, S., Kwak, W., & Kim, H. (2022). Microbial identification using rRNA operon region: Database and tool for metataxonomics with long-read sequence. *Microbiology Spectrum*, *10*(2), e0201721. https://doi.org/10.1128/spectrum.02017-21

Sherrill-Mix, S. (2023). *taxonomizr: Functions to Work with NCBI Accessions and Taxonomy*. https://CRAN.R-project.org/package=taxonomizr

Shim, J., Hong, S. Y., Han, J.-H., Yu, Y., Yoo, E., Sung, J., Chin, J. H., & Lee, O. N. (2023). A genomic evaluation of six selected inbred lines of the naturalized plants of milk thistle (*Silybum marianum* L. Gaertn.) in Korea. *Plants*, *12*(14). https://doi.org/10.3390/plants12142702

Sieracki, M. E., Poulton, N. J., Jaillon, O., Wincker, P., de Vargas, C., Rubinat-Ripoll, L., Stepanauskas, R., Logares, R., & Massana, R. (2019). Single cell genomics yields a wide diversity of small planktonic protists across major ocean ecosystems. *Scientific Reports*, *9*(1), 6025. https://doi.org/10.1038/s41598-019-42487-1

Simon, U. K., & Weiss, M. (2008). Intragenomic variation of fungal ribosomal genes is higher than previously thought. *Molecular Biology and Evolution*, *25*(11), 2251–2254. https://doi.org/10.1093/molbev/msn188

Sonnenberg, R., Nolte, A. W., & Tautz, D. (2007). An evaluation of LSU rDNA D1-D2 sequences for their use in species identification. *Frontiers in Zoology*, *4*(1), 6. https://doi.org/10.1186/1742-9994-4-6

Stoddard, S. F., Smith, B. J., Hein, R., Roller, B. R. K., & Schmidt, T. M. (2015). rrnDB: improved tools for interpreting rRNA gene abundance in bacteria and archaea and a new foundation for future development. *Nucleic Acids Research*, *43*(Database issue), D593-8. https://doi.org/10.1093/nar/gku1201

Stoeck, T., Bass, D., Nebel, M., Christen, R., Jones, M. D. M., Breiner, H.-W., & Richards, T. A. (2010). Multiple marker parallel tag environmental DNA sequencing reveals a highly complex eukaryotic community in marine anoxic water. *Molecular Ecology*, *19 Suppl 1*, 21–31. https://doi.org/10.1111/j.1365-294X.2009.04480.x

Symonová, R. (2019). Integrative rDNAomics-importance of the oldest repetitive fraction of the eukaryote genome. *Genes*, *10*(5), 345. https://doi.org/10.3390/genes10050345

Taberlet, P., Bonin, A., Zinger, L., & Coissac, E. (2018). *Environmental DNA*. Oxford University Press.

Tamura, K., & Nei, M. (1993). Estimation of the number of nucleotide substitutions in the control region of mitochondrial DNA in humans and chimpanzees. *Molecular Biology and Evolution*, *10*(3), 512–526. https://doi.org/10.1093/oxfordjournals.molbev.a040023

Tedersoo, L., Anslan, S., Bahram, M., Kõljalg, U., & Abarenkov, K. (2020). Identifying the 'unidentified' fungi: a global-scale long-read third-generation sequencing approach. *Fungal Diversity*, *103*(1), 273–293. https://doi.org/10.1007/s13225-020-00456-4

Thornhill, D. J., Lajeunesse, T. C., & Santos, S. R. (2007). Measuring rDNA diversity in eukaryotic microbial systems: how intragenomic variation, pseudogenes, and PCR artifacts confound biodiversity estimates. *Molecular Ecology*, *16*(24), 5326–5340. https://doi.org/10.1111/j.1365-294X.2007.03576.x

Tian, M., Hao, L., Li, R., & Zhang, L. (2024). Genome transposon analysis of blackleg causal pathogen. In *Research Square*. https://doi.org/10.21203/rs.3.rs-3987713/v1

Tørresen, O. K., Star, B., Mier, P., Andrade-Navarro, M. A., Bateman, A., Jarnot, P., Gruca, A., Grynberg, M., Kajava, A. V., Promponas, V. J., Anisimova, M., Jakobsen, K. S., & Linke, D. (2019). Tandem repeats lead to sequence assembly errors and impose multi-level challenges for genome and protein databases. *Nucleic Acids Research*, *47*(21), 10994–11006. https://doi.org/10.1093/nar/gkz841

Wang, C., Zhang, T., Wang, Y., Katz, L. A., Gao, F., & Song, W. (2017). Disentangling sources of variation in SSU rDNA sequences from single cell analyses of ciliates: impact of copy number variation and experimental error. *Proceedings. Biological Sciences*, *284*(1859). https://doi.org/10.1098/rspb.2017.0425

White, T. J., Bruns, T., Lee, S., & Taylor, J. (1990). Amplification and direct sequencing of fungal ribosomal RNA genes for phylogenetics. In *PCR Protocols* (pp. 315–322). Elsevier. https://doi.org/10.1016/b978-0-12-372180-8.50042-1

Wickham, H. (2016). *Ggplot2* (2nd ed.) [PDF]. Springer International Publishing.

Wilke, C. O. (2024). *ggridges: Ridgeline Plots in "ggplot2."* https://CRAN.R-project.org/package=ggridges

Wurzbacher, C., Larsson, E., Bengtsson-Palme, J., Van den Wyngaert, S., Svantesson, S., Kristiansson, E., Kagami, M., & Nilsson, R. H. (2019). Introducing ribosomal tandem repeat barcoding for fungi. *Molecular Ecology Resources*, *19*(1), 118–127. https://doi.org/10.1111/1755-0998.12944

Xu, B. (2023). Fungal biotechnology and applications. *Journal of Fungi (Basel, Switzerland)*, *9*(9). https://doi.org/10.3390/jof9090871

Zhao, Y., Wang, Y., Ma, D., Feng, G., Huo, Y., Liu, Z., Zhou, L., Zhang, Y., Xu, L., Wang, L., Zhao, H., Zhao, J., & Wang, F. (2022). A chromosome-level genome assembly and annotation of the maize elite breeding line Dan340. *GigaByte (Hong Kong, China)*, *2022*, gigabyte63. https://doi.org/10.46471/gigabyte.63

Data Accessibility and Benefit-Sharing

The full set (69,480) and the reference set of operon variants (11,867) are available in the ROD database (https://github.com/krabberod/ROD). The release used in this study is ROD v1.1 (GoldenRod), which is also deposited on Zenodo (https://zenodo.org/records/11060492).

Author Contributions

AKK conceived the idea of establishing ROD and assembled the database. AKK and EES did the analyses, HK and AKK drafted the manuscript while all co-authors commented and edited.

Figures

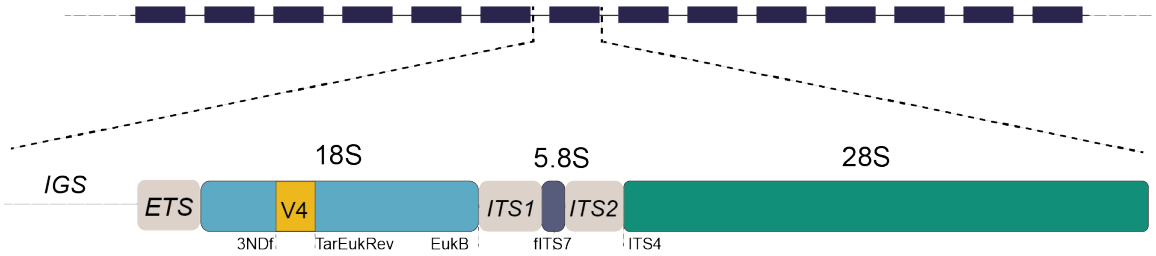

Figure 1. Typical arrangement of the ribosomal operon in eukaryotes. The ribosomal operon is commonly arranged in tandem repeats with intergenic spacers (IGS) between copies and an external transcribed spacer located before the 18S gene. The genes 18S, 5.8S, and 28S are separated by the internally transcribed spacers (ITS1 and ITS2). The binding sites of primers used to separate regions of interest for the clustering analyses are annotated underneath the operon.

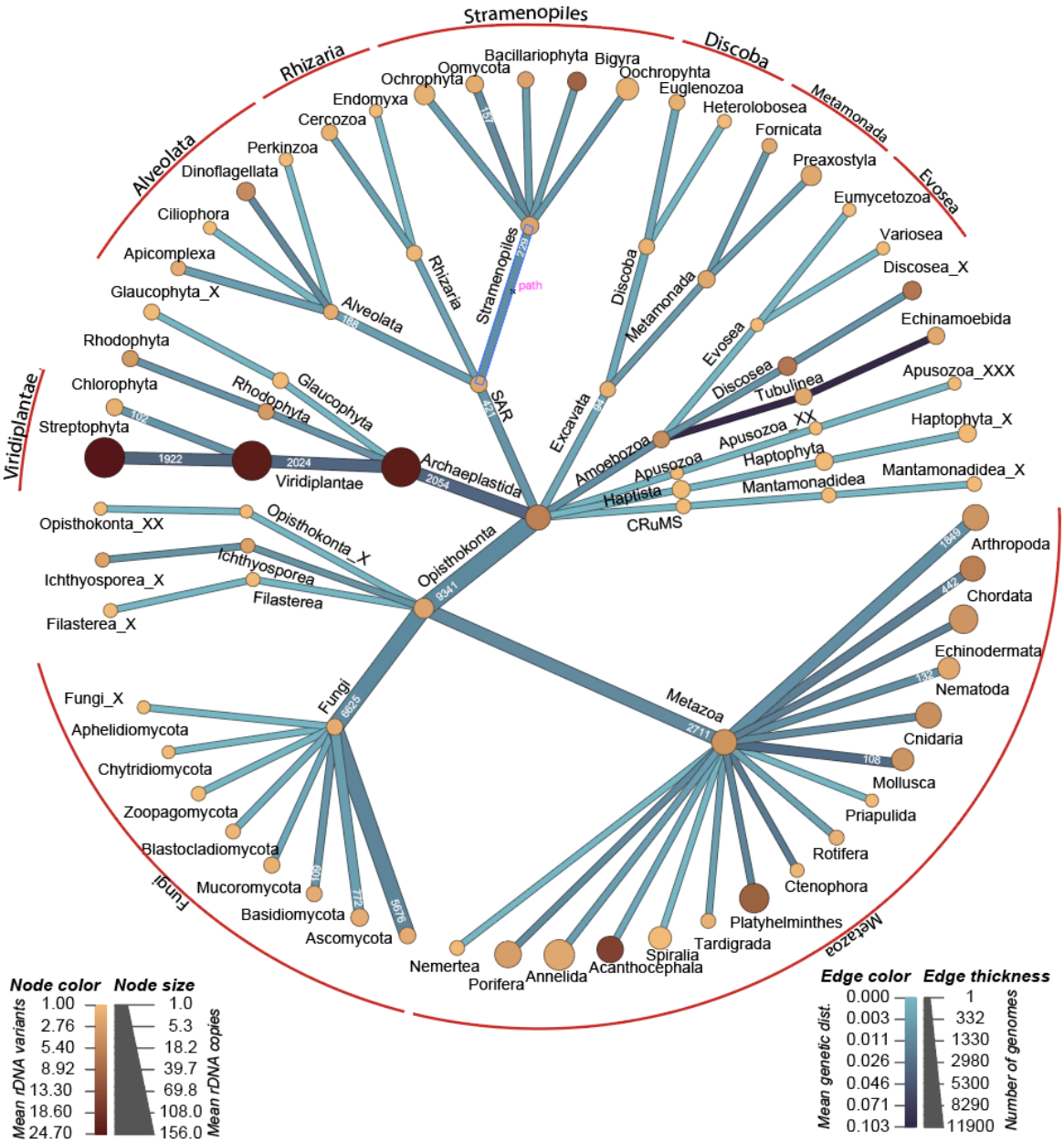

Figure 2. The Distribution of the 69,480 analyzed rDNA operons across the eukaryotic tree of life in the Ribosomal Operon Database (ROD). The unrooted tree is a schematic representation of eukaryotes produced using Metacoder (Foster et al., 2017). The thickness of the branches represents the number of genomes for the clade, and the color of the branches is the weighted genetic distance for the variants. The size of the nodes represents the Mean rDNA copy number for the genomes of that node, and the color of the nodes represents the mean number of variants.

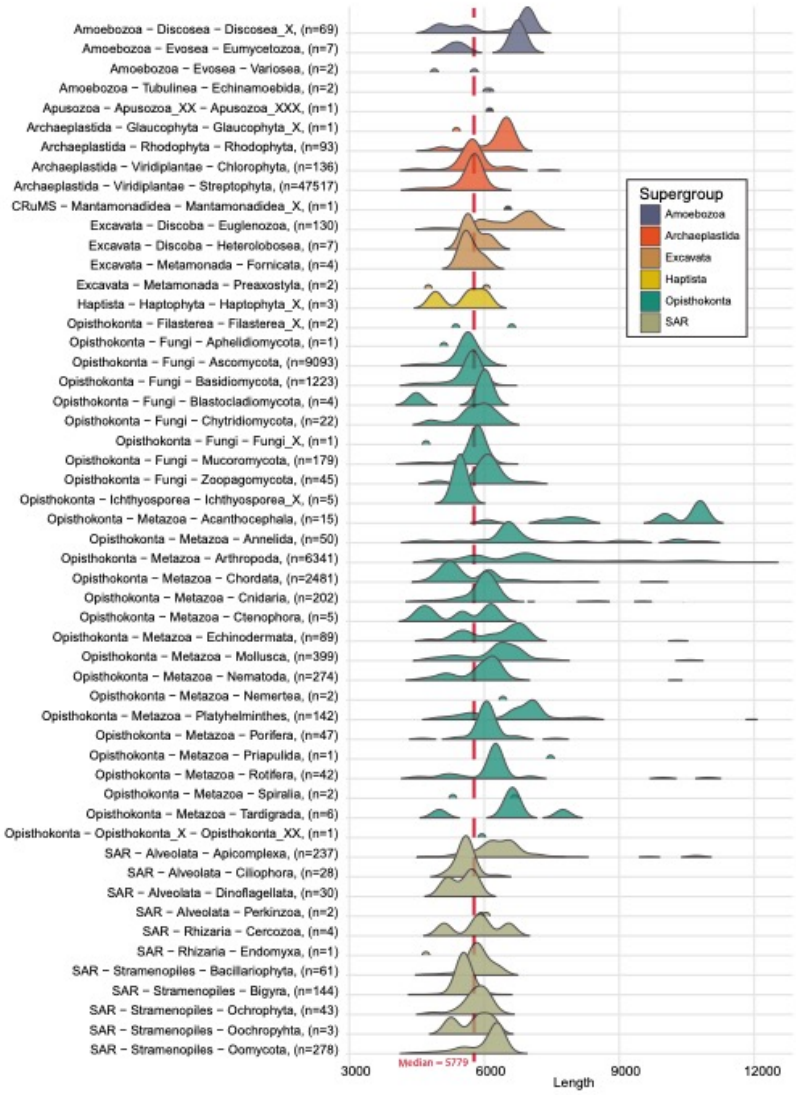

Figure 3. Length distribution of the recorded rDNA operons across the eukaryotic subdivisions in the Ribosomal Operon Database (ROD). The ridge plot represents the density distribution of lengths within each group. The number of genomes for each subdivision is written in parentheses. The median length is recorded as a red dashed line.

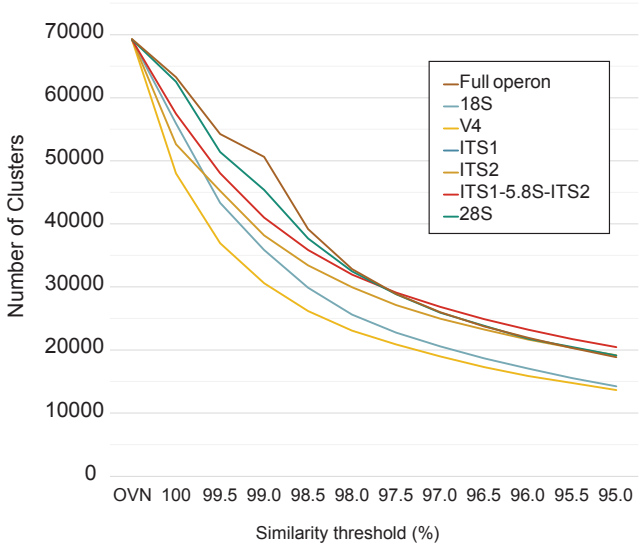

625

626 **Figure 4**. **Cluster analysis of the 69,480 full-length operon variants in ROD and different sub-parts**
627 **commonly used in DNA metabarcoding studies.** The number of sequence clusters (y-axis) plotted against
628 the clustering threshold for the entire operon, as well as the different subparts. On the x-axis, OVN is the
629 original variant number, i.e., the number of operons before clustering (69,480), while 100% gives the
630 number of variants after collapsing identical operon variants across all genomes, similar to a dereplication.

Table 1. Characteristics of rDNA operon in eukaryotes for each subdivision. Detailed statistics of ribosomal operons extracted from eukaryotic genomes in NCBI, categorized by Supergroup, Division, and Subdivision. Each entry provides data on the number of genomes analyzed for each subdivision, operon copy number statistics (mean and maximum), variant counts, average genetic distance, and operon length metrics (minimum, maximum, mean). The number of operon variants is defined as sequences at least 1% dissimilar, and the average genetic distance is calculated based on the variants and weighted by the number of copies per variant. *Genomes*: Number of genomes examined for the particular subdivision. *Avg. copy number*: Average number of ribosomal operon copies per genome in the subdivision. *Max Copies*: Maximum number of operon copies found in a single genome within the category. *Max Variants:* Maximum number of operon variants found among the genomes in the subdivision.*Avg. variants*: Average number of operon variants within the subdivision. *Min/Max/Avg Operon Length*: The minimum, maximum, and average length of operons within each subdivision, expressed in base pairs (bp). Cells containing '-' indicate data not available or not applicable for specific categories.

Supergroup	*Division*	*Subdivision*	*Genomes*	*Avg. copy number*	*Max copies*	*Max. variants*	*Avg. variants*	*Avg. genetic distance*	*Min. operon length*	*Max. operon length*	*Avg. operon length*
Amoebozoa	Discosea	Discosea_X	10	59	11.3	36	6.9	0.006	4,814	7,027	5,765
Amoebozoa	Evosea	Eumycetozoa	7	2	1.1	1	1.0	-	5,260	6,837	6,362
Amoebozoa	Evosea	Variosea	2	1	1.0	1	1.0	-	4,891	5,778	5,335
Amoebozoa	Tubulinea	Echinamoebida	1	8	8.0	2	2.0	0.103	6,055	6,125	6,125
Apusozoa	Apusozoa_XX	Apusozoa_XXX	1	1	1.0	1	1.0	-	6,118	6,118	6,118
Archaeplastida	Glaucophyta	Glaucophyta_X	1	5	5.0	1	1.0	-	5,381	5,381	5,381
Archaeplastida	Rhodophyta	Rhodophyta	29	21	5.7	10	3.2	0.006	4,694	6,634	6,073
Archaeplastida	Viridiplantae	Streptophyta	1,922	5,947	155.8	2,097	24.7	0.033	4,136	13,249	5,645
Archaeplastida	Viridiplantae	Chlorophyta	102	112	7.1	6	1.3	0.005	4,347	7,448	5,695
CRuMS	Mantamonadidea	Mantamonadidea_X	1	3	3.0	1	1.0	-	6,527	6,527	6,527
Excavata	Discoba	Euglenozoa	84	36	4.8	11	1.5	0.001	4,684	7,448	6,627
Excavata	Discoba	Heterolobosea	7	6	1.9	1	1.0	-	5,605	6,105	5,766
Excavata	Metamonada	Fornicata	2	6	3.5	3	2.0	0.004	5,580	5,975	5,778
Excavata	Metamonada	Preaxostyla	1	17	17.0	2	2.0	0.003	4,757	6,047	4,757
Haptista	Haptophyta	Haptophyta_X	3	20	9.7	1	1.0	-	4,915	6,020	5,535
Opisthokonta	Filasterea	Filasterea_X	2	3	2.0	1	1.0	-	5,367	6,611	5,989
Opisthokonta	Fungi	Ascomycota	5,676	1,078	6.1	81	1.6	0.012	4,185	6,905	5,595
Opisthokonta	Fungi	Basidiomycota	772	463	8.9	26	1.6	0.003	4,272	6,691	5,632
Opisthokonta	Fungi	Mucoromycota	109	68	4.9	5	1.6	0.005	4,263	6,646	5,692
Opisthokonta	Fungi	Zoopagomycota	41	49	3.0	4	1.1	0.000	4,855	7,105	6,090
Opisthokonta	Fungi	Chytridiomycota	22	11	2.6	1	1.0	-	4,787	6,409	5,803
Opisthokonta	Fungi	Blastocladiomycota	3	8	5.3	2	1.3	0.001	4,486	6,058	6,013
Opisthokonta	Fungi	Fungi_X	1	1	1.0	1	1.0	-	4,706	4,706	4,706
Opisthokonta	Fungi	Aphelidiomycota	1	5	5.0	1	1.0	-	5,102	5,102	5,102
Opisthokonta	Ichthyosporea	Ichthyosporea_X	2	4	2.5	4	2.5	0.006	5,407	5,486	5,446
Opisthokonta	Metazoa	Arthropoda	1,849	4,691	42.1	139	3.4	0.008	4,395	16,463	6,685
Opisthokonta	Metazoa	Chordata	442	1,007	38.3	665	5.6	0.015	4,162	13,305	5,370

Opisthokonta	Metazoa	Nematoda	132	448	23.3	15	2.1	0.007	4,415	10,248	5,972
Opisthokonta	Metazoa	Mollusca	108	505	24.9	96	3.7	0.027	4,640	11,390	6,384
Opisthokonta	Metazoa	Cnidaria	49	880	41.2	40	4.1	0.008	4,409	10,417	5,936
Opisthokonta	Metazoa	Rotifera	33	25	3.3	4	1.3	0.002	4,453	10,979	6,228
Opisthokonta	Metazoa	Echinodermata	26	710	58.9	45	3.4	0.014	4,772	10,310	5,865
Opisthokonta	Metazoa	Annelida	26	646	72.5	6	1.9	0.003	4,440	10,955	6,612
Opisthokonta	Metazoa	Porifera	18	258	47.0	8	2.6	0.009	4,624	7,588	5,960
Opisthokonta	Metazoa	Platyhelminthes	14	679	63.7	76	10.1	0.011	4,910	11,943	6,426
Opisthokonta	Metazoa	Ctenophora	4	4	2.0	2	1.3	0.016	4,558	6,236	5,275
Opisthokonta	Metazoa	Tardigrada	4	3	3.0	3	1.5	0.002	5,000	7,748	6,246
Opisthokonta	Metazoa	Spiralia	2	49	26.5	1	1.0	-	5,300	6,675	5,988
Opisthokonta	Metazoa	Nemertea	2	4	3.0	1	1.0	-	6,413	6,415	6,414
Opisthokonta	Metazoa	Priapulida	1	1	1.0	1	1.0	-	7,473	7,473	7,473
Opisthokonta	Metazoa	Acanthocephala	1	46	46.0	15	15.0	0.001	6,064	10,883	10,776
Opisthokonta	Opisthokonta_X	Opisthokonta_XX	1	1	1.0	1	1.0	-	5,946	5,946	5,946
SAR	Alveolata	Apicomplexa	151	59	3.3	30	1.6	0.003	4,647	10,794	6,338
SAR	Alveolata	Ciliophora	28	3	1.1	1	1.0	-	5,209	6,274	5,584
SAR	Alveolata	Dinoflagellata	7	33	11.0	13	4.3	0.010	5,078	5,844	5,509
SAR	Alveolata	Perkinzoa	2	2	1.5	1	1.0	-	5,936	6,044	5,990
SAR	Rhizaria	Cercozoa	3	6	5.3	2	1.3	0.002	5,107	6,545	6,118
SAR	Rhizaria	Endomyxa	1	1	1.0	1	1.0	-	4,702	4,702	4,702
SAR	Stramenopiles	Oomycota	157	72	9.0	15	1.8	0.008	4,261	7,317	6,054
SAR	Stramenopiles	Ochrophyta	28	376	17.6	7	1.5	0.003	4,799	6,383	5,897
SAR	Stramenopiles	Bacillariophyta	27	24	5.7	13	2.3	0.003	4,713	6,401	5,795
SAR	Stramenopiles	Bigyra	15	102	11.3	87	9.6	0.003	4,436	6,489	5,664
SAR	Stramenopiles	Oochropyhta	2	48	24.5	2	1.5	0.004	5,262	6,164	5,554